Conformational Transition of Tethered Poly(*N*-isopropylacrylamide) Chains in Coronas of Micelles and Vesicles

Weian Zhang, Xuechang Zhou, Hao Li, Yueer Fang, and Guangzhao Zhang*

Hefei National Laboratory for Physical Sciences at Microscale, Department of Chemical Physics, Department of Polymer Science & Engineering, University of Science and Technology of China, Hefei, Anhui, China

Received August 30, 2004; Revised Manuscript Received November 19, 2004

ABSTRACT: Thermosensitive micelles and vesicles in water were prepared using narrowly distributed polystyrene-*b*-poly(*N*-isopropylacrylamide) (PS-*b*-PNIPAM) diblock copolymers, and the conformational changes of PNIPAM blocks in the coronas of micelles and vesicles were investigated by a combination of static and dynamic laser light scattering. Our results reveal that PNIPAM chains forming brushes in the corona of the micelles undergo a continuous collapse transition, which is consistent with the theoretical predictions. PNIPAM brushes in the coronas of the vesicles exhibit a broad transition from 28 to 36 °C with a shrinking in the range 20−28 °C. The shrinking at a low temperature is attributed to the interchain overlapping of the dense brushes on the concave surface of the vesicle. On the other hand, the vesicles become hollow with temperature increasing because of the collapse of the PNIPAM chains in the inside corona of the vesicle.

Introduction

Since Stockmayer[1] first proposed that a flexible polymer chain can undergo a transition from an expanded coil to a collapsed globule on the basis of Flory's mean-field theory,[2] coil-to-globule transition of a synthetic polymer chain has been investigated both theoretically[3−11] and experimentally[12−23] because it has important implications for protein folding and DNA packing. Poly(*N*-isopropylacrylamide) (PNIPAM) exhibits a lower critical solution temperature (LCST) at ∼32 °C in aqueous solution,[24] and its conformation change is conveniently realized by adjusting temperature. Accordingly, PNIPAM-based polymer chains free in solution have been preferable for such a study.[17−23]

On the other hand, when polymer chains are grafted by one end onto a surface, they show a conformation much different from that of free chains depending on the grafting density; namely, each chain behaves like a free chain with a random coil conformation at a low grafting density. As the grafting density increases, the grafted chains swollen in good solvent are stretching out to form a polymer brush without any overlapping due to the effect of exclusion.[25−28] The strong interchain interactions are predicted to broaden the coil-to-globule transition.[29] Such end-grafted polymer brushes chains have found a number of applications in colloidal stabilization,[30] tissue culture,[31] drug delivery,[32] tribology,[33] and bacteria.[34] So far, experimental investigations on the conformational change of polymer brushes are still limited,[35−42] and some of them are disputed. Static density profile and dynamic measurements reveal that polystyrene brush on a planar surface exhibits a continuous collapse with decreasing solvency.[35,36] Similarly, PNIPAM brushes on a planar gold surface were found to undergo a quite broad transition.[37] PNIPAM chains attached on polystyrene latex particles also show a phase transition wider than the coil-to-globule transition of PNIPAM chains free in water.[38] All the experimental results agree with the theoretical predictions.[29] In contrast, the contact angle measurements revealed that PNIPAM brush has a sharp solubility transition at ∼32 °C.[41,42]

It should be noted that even linear PNIPAM chains physically adsorbed on the surface of polystyrene nanoparticles[43] or flat surface[44] also show a broad coil-to-globule transition, indicating that the surface properties and polymer−surface interactions also influence the conformation change of the tethered polymer chains. In the present study, we prepared micelles and vesicles with narrowly distributed polystyrene-*b*-poly(*N*-isopropylacrylamide) (PS-*b*-PNIPAM) diblock copolymers, where PNIPAM blocks consist of their coronas. The temperature-induced conformational changes of PNIPAM chains tethered on convex and concave surfaces were investigated.

Experimental Section

Styrene was first washed with an aqueous solution of sodium hydroxide (5 wt %) three times and with water until neutralization and then distilled under reduced pressure. *N*-Isopropylacrylamide (NIPAM, Aldrich) was purified by recrystallization from a mixture of benzene and *n*-hexane. 4,4′-Azobis(isobutyronitrile) (AIBN) (Fluka, 98%) were purified by recrystallization from ethanol. Tetrahydrofuran (THF) was distilled from a purple sodium ketyl solution. Other reagents were used as received without further purification.

^{1}H NMR spectra were measured on a Bruker DMX-500 NMR spectrometer using chloroform-*d* ($CDCl_3$) as the solvent and tetramethylsilane (TMS) as the internal standard. Molecular weights were determined by gel permeation chromatography (GPC) on a Waters 150C using monodisperse polystyrene as the calibration standard and THF as the eluent with a flow rate of 1.0 mL/min.

Synthesis of PS-*b*-PNIPAM. The procedures for synthesis of chains transfer agent and polystyrene (PS) terminated with dithiobenzoate (PhC(S)S) can be found elsewhere in detail.[40,45] Styrene (5.138 g, 49.3 mmol), AIBN (4.0 mg, 0.024 mmol), and DTBA (33.0 mg, 0.135 mmol) were added into a 10 mL glass tube. After three freeze−vacuum−thaw cycles, the tube was sealed under vacuum and then placed in a thermostated bath

* To whom correspondence should be addressed.

10.1021/ma048227s CCC: $30.25
Published on Web 01/14/2005

at 68 °C for 24 h. The resulting PS was precipitated into ethanol, filtered, and then dried in a vacuum oven at 40 °C for 24 h. Finally, 2.485 g of PS terminated with dithiobenzoate (PS−PhC(S)S) was obtained. ^{1}H NMR (500 MHz, $CDCl_3$), δ (TMS, ppm): 7.85 [ortho *Ph*C(S)S), 7.32−6.30 (aromatic protons), 2.21−1.29 (*CH*$_2$*CH*). M_n(GPC) = 21 500; M_w/M_n(GPC) = 1.07.

A typical diblock copolymer was synthesized as follows. PS−PhC(S)S (0.409 g), NIPAM (0.581 g), AIBN (1.0 mg), and THF (4 mL) were added into a 10 mL glass tube. After three freeze−vacuum−thaw cycles, the tube was sealed under vacuum and then placed in a thermostat bath at 68 °C for 16 h. The polymer was precipitated into petroleum ether (bp 30−60 °C). Precipitation was repeated three times, and the polymer was dried at 40 °C in a vacuum oven for 24 h. In this way, 0.601 g of PS-*b*-PNIPAM was obtained. Block copolymers with a longer PNIPAM block was synthesized with the same procedure except that more NIPAM was added. ^{1}H NMR (500 MHz, $CDCl_3$), δ (TMS, ppm): 7.85 [ortho *Ph*C(S)S), 7.32−6.30 (aromatic protons), 4.04 [NH*CH*(CH$_3$)$_2$], 2.42−1.29 (*CH*$_2$*CH*CO, *CH*$_2$*CH*), 1.20 (NHCH(*CH*$_3$)$_2$). Molecular weights of the diblock copolymers were calculated from the intensities of the characteristic peaks in ^{1}H NMR together with the molecular weight of PS block measured by GPC. For PS(207)-*b*-PNIPAM(176) containing 207 styrene units and 176 NIPAM units, M_w/M_n = 1.20. For PS(207)-*b*-PNIPAM(357) with a longer PNIPAM block, M_w/M_n = 1.17.

Preparation of Aggregates. A "T" shape springe mixer with three channels and a Sp100i springe pump was used to prepare the aggregates. PS-*b*-PNIPAM solution in THF and Milli-Q water flowed into the springe mixer through two channels at 20 °C with rates of 50 and 400 mL/h, respectively, joined and flowed out through the other channel. As the mixing progressed in such a way, the insoluble PS blocks gradually contracted and associated, while soluble PNIPAM blocks tended to stay on the periphery, leading to micelle-like aggregates. The resulting solution was dialyzed against Milli-Q water using a semipermeable membrane with cutoff molar masses of 7000 g/mol for 3 days to remove all of the THF.

High-Resolution Transmission Electron Microscopy (HTEM). The morphologies of the aggregates were observed on a JEOL2100 high-resolution transmission electron microscope operating at an acceleration voltage of 200 kV. A drop of the dilute aqueous solution with a concentration of 1.0 × 10^{-4} g/mL was deposited onto a carbon-coated copper mesh grid. Two minutes after the deposition, the samples were used for HTEM studies.

Laser Light Scattering. A commercial LLS spectrometer (ALV/DLS/SLS-5022F) equipped with a multi-τ digital time correlation (ALV5000) and a cylindrical 22 mW UNIPHASE He−Ne laser (λ_0 = 632 nm) as the light source was used. In static LLS,[46,47] the angular dependence of the absolute excess time-average scattering intensity was known as the Rayleigh ratio $R_{vu}(q)$, and we were able to obtain the weight-average molar mass (M_w), the root-mean-square radius of gyration $\langle R_g^2\rangle_z^{1/2}$ (or written as $\langle R_g\rangle$), and the second virial coefficient A_2 by using

$$\frac{KC}{R_{vv}(q)} \approx \frac{1}{M_w}\left(1 + \frac{1}{3}\langle R_g^2\rangle_z q^2\right) + 2A_2C \qquad (1)$$

where $K = 4\pi^2(dn/dC)^2/(N_A\lambda_0^4)$ and $q = (4\pi n/\lambda_0)\sin(\theta/2)$ with C, dn/dC, N_A, and λ_0 being concentration of the polymer, the specific refractive index increment, the Avogadro number, and the wavelength of light, respectively. In dynamic LLS,[48] the intensity−intensity time correlation function $G^{(2)}(t,q)$ in the self-beating mode was measured. $G^{(2)}(t,q)$ can be related to the normalized first-order electric field−electric field time correlation function ($|g^{(1)}(t,q)| \equiv \langle E(0,q)\, E(t,q)\rangle$) as

$$G^{(2)}(t,q) = \langle I(0,q)\, I(t,q)\rangle = A[1 + \beta|g^{(1)}(t,q)|^2] \qquad (2)$$

where t is the delay time, A is the measured baseline, and β is an instrument constant depending on the optical coherence

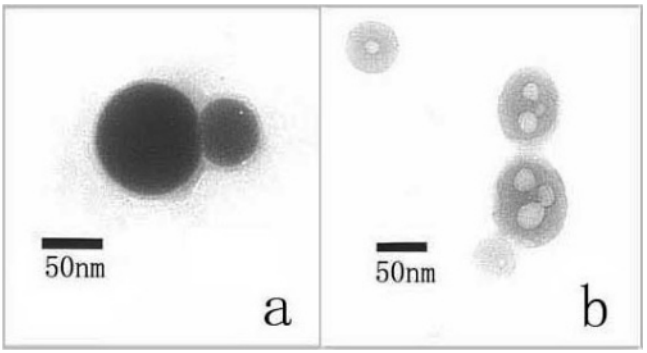

Figure 1. HTEM imagines of the aggregates at 25 °C: (a) PS(207)-*b*-PNIPAM(357) and (b) PS(207)-*b*-PNIPAM(176), where where $C = 1.0 \times 10^{-4}$ g/mL.

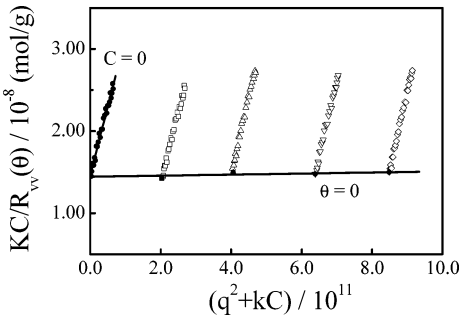

Figure 2. Typical Zimm plot for PS(207)-*b*-PNIPAM(176) aggregates in water at 25 °C, where concentration ranges from 5.03×10^{-6} to 2.10×10^{-5} g/mL.

of the detection. In general, $|g^{(1)}(t,q)|$ is related to a characteristic line-width distribution $G(\Gamma)$ as

$$|g^{(1)}(t,q)| = \int G(\Gamma)e^{-\Gamma t}\, d\Gamma \qquad (3)$$

For diffusive relaxation, Γ is related to the translational diffusion coefficient (D) of the scattering object (polymer chain or colloid particle) in dilute solution or dispersion by

$$\Gamma/q^2 = D(1 + Cq^2\langle R_g^2\rangle + ...) \qquad (4)$$

where coefficient C depends on the structure and hydrodynamic interactions of the scattering object. Equation 4 yields $(\Gamma/q^2)_{q\to 0, C\to 0} = D$. Hydrodynamic radius ($R_h$) is obtained by the Stokes−Einstein equation: $R_h = k_BT/(6\pi\eta D)$, where η, k_B, and T are the solvent viscosity, the Boltzmann constant, and the absolute temperature, respectively. For a narrowly distributed system, the cumlant analysis of $|g^{(1)}(t,q)|$ is sufficient to generate in a reliable average $\langle\Gamma\rangle$ or $\langle D\rangle$ or $\langle R_h\rangle$. The hydrodynamic radius distribution $f(R_h)$ was calculated from the Laplace inversion of a corresponding measured $G^{(2)}(t,q)$ using the CONTIN program in the correlator on the basis of eqs 1−3. All the dynamic LLS results were obtained at a small scattering angle of 15°. The refractive index increments of the polymeric aggregates were calculated using an addition method.[49]

Results and Discussion

Figure 1 shows typical HTEM images of aggregates prepared from PS(207)-*b*-PNIPAM(357) and PS(207)-*b*-PNIPAM(176) diblock copolymers. The former yields spherical micelles with a core−shell structure (Figure 1a). On the other hand, the latter with a shorter PNIPAM block form vesicles (Figure 1b).[50] It can be seen some aggregates fuse together with the evaporation of the solvent.

Figure 2 shows a typical Zimm plot for PS(207)-*b*-PNIPAM(176) vesicles at 25 °C. On basis of eq 1, the

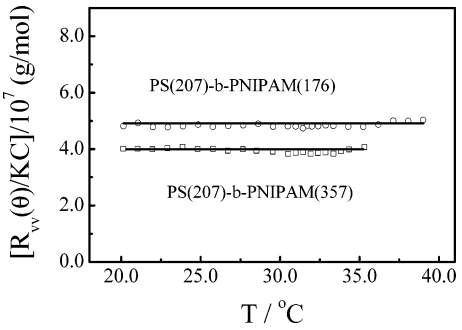

Figure 3. Temperature dependence of the excess scattering intensity ($R_{vv}(\theta)/KC$) of PS(207)-*b*-PNIPAM(176) and PS(207)-*b*-PNIPAM(357) aggregates, where $C = 1.0 \times 10^{-4}$ g/mL.

molar mass (M_w), average radius of gyration ($\langle R_g \rangle$), and the second virial coefficient (A_2) of PS(207)-*b*-PNIPAM-(176) vesicles are determined to be 6.9×10^7 g/mol, 59.8 nm, and 1.7×10^{-5} mol cm^3/g^2. Similarly, for PS(207)-*b*-PNIPAM(357) micelles, we have $M_w = 6.1 \times 10^7$ g/mol, $\langle R_g \rangle = 68.3$ nm, and $A_2 = 1.5 \times 10^{-4}$ mol cm^3/g^2. The positive and small values of A_2 suggest that water is a selective solvent for both PS(207)-*b*-PNIPAM(176) and PS(207)-*b*-PNIPAM(357). On the other hand, PS(207)-*b*-PNIPAM(357) has a higher A_2 than PS(207)-*b*-PNIPAM(176), indicating that the former is more hydrophilic than the latter. This is understandable because PS(207)-*b*-PNIPAM(357) has a longer hydrophilic PNIPAM block than PS(207)-*b*-PNIPAM(176).

Figure 3 shows the temperature dependence of the excess scattering intensity $R_{vv}(\theta)/KC$ of PS(207)-*b*-PNIPAM(176) and PS(207)-*b*-PNIPAM(357) aggregates. Since $R_{vv}(\theta)/KC$ is proportional to the weight-average molar mass ($M_{w,agg}$) of the aggregates on the basis of eq 1, it is sensitive to the aggregation. The temperature independence of $R_{vv}(\theta)/KC$ clearly indicates that neither the micelles nor the vesicles aggregate when temperature is lower than a certain value called aggregation temperature (T_{agg}). For PS(207)-*b*-PNIPAM(357) micelles and PS(207)-*b*-PNIPAM(176) vesicles, T_{agg}s are ~36 and ~40 °C, respectively. In other words, they show an individual behavior at a temperature below T_{agg}. When temperature is above T_{agg}, the micelles or vesicles gradually aggregate. Obviously, the tethered PNIPAM chains are much more stable than free PNIPAM chains which quickly aggregate at ~32 °C. The phenomenon was also recently observed by Tenhu et al.[40] This is because the tethered chains have much smaller contact area than the free chains, and they have less chances to stick together. This is further confirmed by the fact that PS(207)-*b*-PNIPAM(176) vesicles are more stable than PS(207)-*b*-PNIPAM(357) micelles since the former with shorter PNIPAM block have smaller contact area than the latter.

Figure 4 shows the temperature dependence of average hydrodynamic radius $\langle R_h \rangle$ and average radius of gyration $\langle R_g \rangle$ of PS(207)-*b*-PNIPAM(357) micelles. Each data point was obtained after the measured values were stable. It can be seen that both $\langle R_h \rangle$ and $\langle R_g \rangle$ gradually decrease with the temperature, exhibiting a broad transition from ~25 to 33 °C. In contrast, individual PNIPAM chains free in solution showed a sharp decrease of the overall chain size in a very narrow temperature range 30−32 °C.[18] Our results here are consistent with the coil-to-globule transition of PNIPAM chains attached on PS latex.[38] The $\langle R_h \rangle$ drops ~16 nm after the micelles shrink from their swollen state at 20

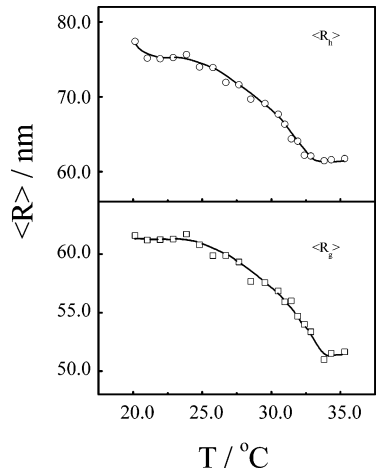

Figure 4. Temperature dependence of average hydrodynamic radius $\langle R_h \rangle$ and average radius of gyration $\langle R_g \rangle$ of PS(207)-*b*-PNIPAM(357) micelles, where $C = 1.0 \times 10^{-4}$ g/mL.

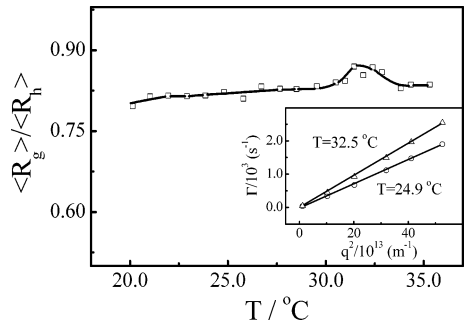

Figure 5. Temperature dependence of the ratio of average hydrodynamic radius to average radius of gyration ($\langle R_g \rangle/\langle R_h \rangle$) of PS(207)-*b*-PNIPAM(357) micelles, where $C = 1.0 \times 10^{-4}$ g/mL.

°C to the most collapsed state. However, in our preliminary experiments, we found that the $\langle R_h \rangle$ of a free PNIPAM chain with a molecular weight ~4×10^4 g/mol is less than 5 nm. The facts indicate PNIPAM blocks in PS(207)-*b*-PNIPAM(357) micelles are stretched. This can be better viewed in terms of the occupied area (σ) per PNIPAM block on PS core.

The occupied area (σ_m) per PNIPAM chain on the spherical surface of micelle with a radius of R at most collapsed state is calculated to be 47 nm^2 using $\sigma_m = 4\pi R^2/N$, where $R = 61$ nm and the aggregation number (N) is 986. The thickness change (ΔH) of PNIPAM brushes is ~16 nm (Figure 4), so we have $\Delta H > \sigma_m^{0.5}$. Since the radius of PS core is smaller than that of the collapsed micelle, the occupied area (σ) per PNIPAM chain on PS core is much smaller than σ_m. Meanwhile, the thickness (H) of PNIPAM corona is much larger than ΔH. Therefore, $H > \sigma^{0.5}$, and PNIPAM blocks form brushes.[25,26]

Figure 5 shows the temperature dependence of $\langle R_g \rangle/\langle R_h \rangle$ of PS(207)-*b*-PNIPAM(357) aggregates. It is known that the ratio $\langle R_g \rangle/\langle R_h \rangle$ can reflect the conformation of a polymer or the structure of a particle. For uniform nondraining sphere, hyperbranched cluster, and random coil, $\langle R_g \rangle/\langle R_h \rangle$ is ~0.774, 1.0−1.2, and 1.5−1.8, respectively;[51,52] a micelle generally has a $\langle R_g \rangle/\langle R_h \rangle \sim 0.8-1.1$. The $\langle R_g \rangle/\langle R_h \rangle \sim 0.8-0.87$ shown in Figure 5 further indicates that PS(207)-*b*-PNIPAM(357) chains form a relatively uniform and slightly draining spherical micelle; i.e., PNIPAM corona has a density close to that of PS core. The linear relation of $\Gamma \sim q^2$ shown in the inset

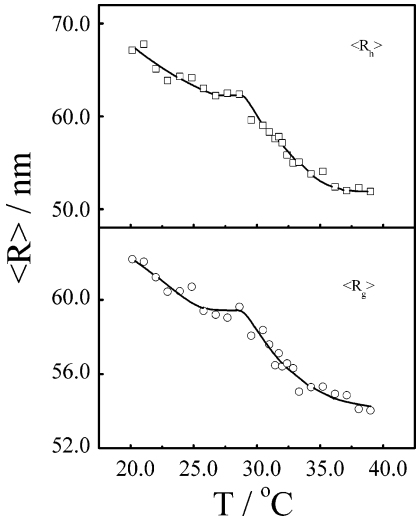

Figure 6. Temperature dependence of $\langle R_h \rangle$ and $\langle R_g \rangle$ of PS(207)-*b*-PNIPAM(176) vesicles, where $C = 1.0 \times 10^{-4}$ g/mL.

indicates that the micelles have an isotropic diffusive behavior in terms of eq 4; i.e., the micelles have a spherical structure. The small fluctuation of $\langle R_g \rangle / \langle R_h \rangle$ indicates the shape of the micelle almost does not change during the heating process. The slight increase of $\langle R_g \rangle / \langle R_h \rangle$ in the range 31−33 °C is attributed to the stressed loops formed during the early stage of the collapse of PNIPAM chains, which hydrodynamically influence $\langle R_h \rangle$ but have little effect on $\langle R_g \rangle$ since $\langle R_g \rangle$ is related to the chain density distribution in space. In the range 31−33 °C, the loops begin to collapse, leading to a more dramatic drop of $\langle R_h \rangle$ as shown in Figure 4, so that $\langle R_g \rangle / \langle R_h \rangle$ slightly increases. A similar phenomenon was also observed in the coil-to-globule transition of single PNIPAM chain.[18]

Figure 6 shows the temperature dependence of $\langle R_h \rangle$ and $\langle R_g \rangle$ of PS(207)-*b*-PNIPAM(176) vesicles. As temperature increases, $\langle R_h \rangle$ and $\langle R_g \rangle$ decrease with a discontinuous transition; namely, $\langle R_h \rangle$ and $\langle R_g \rangle$ slowly decrease in the range 20−28 °C but faster drop over a range from 28 to 36 °C. The latter is due to the collapse of PNIPAM chains. However, the former contrasts the behaviors of PNIPAM chains in PS(207)-*b*-PNIPAM(357) micelles and those grafted on PS latex,[38] where almost no shrinking of PNIPAM chains occurs at a low temperature. On the other hand, Balamurugan et al.[37] observed such a shrinking for PNIPAM brushes grafted on a planar surface with a very broad transition from ~10 to 40 °C. The origin of the shrinking at low temperature is not clear yet. To understand the phenomenon, it may be helpful to consider the curvature of the grafted surface.

Figure 7 shows the $\langle R_g \rangle / \langle R_h \rangle$ of PS(207)-*b*-PNIPAM(176) vesicles increases from ~0.92 to 1.05 with temperature increasing. As discussed above, the $\langle R_g \rangle / \langle R_h \rangle$ values are another evidence that PS(207)-*b*-PNIPAM(176) chains form vesicles with a spherical structure. The isotropic diffusive behavior revealed in the inset also indicates the spherical structure of the vesicles. The larger $\langle R_g \rangle / \langle R_h \rangle$ values imply that the vesicles are less uniform than PS(207)-*b*-PNIPAM(357) micelles. Moreover, the nonuniformity of the vesicles increases with temperature. On the other hand, Figures 4 and 6 indicate that both PS(207)-*b*-PNIPAM(176) vesicles and PS(207)-*b*-PNIPAM(357) micelles have a decrease in $\langle R_h \rangle$ ~16 nm when they shrink from the swollen state

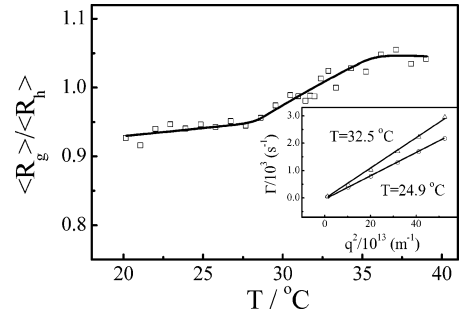

Figure 7. Temperature dependence of the ratio of average hydrodynamic radius to average radius of gyration ($\langle R_g \rangle / \langle R_h \rangle$) of PS(207)-*b*-PNIPAM(176) vesicles, where $C = 1.0 \times 10^{-4}$ g/mL.

to the most collapsed state. As the length of the PNIPAM block in the latter is twice of that in the former, this fact further indicates that PS(207)-*b*-PNIPAM(176) chains form a vesicle with two PNIPAM layers. Assume that the number of chains packing in outside corona of the vesicle is the same as that in the inside corona, we can calculate the thickness change (ΔH) of the outside corona to be ~8 nm and the occupied area (σ_m) per PNIPAM chain in the outside corona at most collapsed state to be ~40 nm^2 using $\sigma_m = 4\pi R^2/N$ with $R = 67$ nm and $N = 1666$, so that $\Delta H > \sigma_m^{0.5}$. As discussed above, we have $H > \sigma^{0.5}$, where H and σ are the thickness of PNIPAM chains in the outside corona and the occupied area per PNIPAM chain on the outside PS surface, so PNIPAM chains in the outside corona can form brushes. PNIPAM chains in the *inside* corona are expected to form brushes since such a concave surface with a much smaller radius leads PNIPAM chains there to be even denser.

Zhulina et al.[29] predicted that the transition of polymer brushes on spherical or cylindrical surfaces has a second-order character, but it is broader than that of free polymer chain, while brushes on a planar surface do not show a phase transition due to the strong interchain interactions. The predictions were tested valid in some experiments. Neutron reflectivity measurements and evanescent wave dynamic light scattering studies indicate that polystyrene brushes on a planar surface exhibit a continuous collapse.[35,36] Surface plasmon resonance investigation also revealed that PNIPAM brushes on a planar gold surface undergo a broad transition.[37] In the present study, very strong interchain interactions among PNIPAM chains in the inside corona are expected because the concave surface makes them have an inherent tendency to overlap even at a very low temperature. The interchain overlapping and entangling reduce the contacts between water and PNIPAM chains, causing the dehydration of the chains at a low temperature. That is why $\langle R_h \rangle$ and $\langle R_g \rangle$ gradually decrease in the range 20−28 °C (Figure 6). Note that PNIPAM chains on the convex surface of the outside corona have little effect on the changes of $\langle R_h \rangle$ and $\langle R_g \rangle$ since they do not have an enough density for the overlapping at a low temperature. Actually, the interchain overlapping and entangling are similar to the intrachain crumpling in the folding of a single PNIPAM chain, which also causes a shrinking of the chain at low temperatures.[18] In our opinion, the shrinking of PNIPAM brushes on a *planar* surface at low temperatures is due to the interchain overlapping.[37] Tethered PNIPAM chains in PS(207)-*b*-PNIPAM(357) micelles in the present study and those on PS latex[38] do not exhibit such a

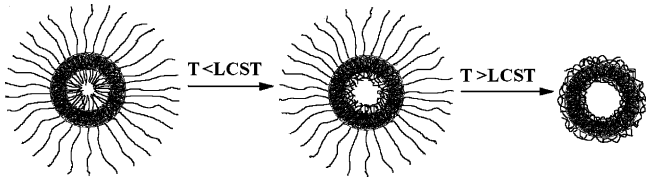

Figure 8. Schematic illustration of collapse of PNIPAM brushes in the coronas of a vesicle.

shrinking because they are not dense enough for the overlapping at a low temperature. It should be noted that tethered PNIPAM chains with a low density forming a mushroom structure may also show a shrinking at a low temperature because they can overlap and entangle behaving like deformed coils. Therefore, only those tethered chains which are stretched but have a relatively low density are expected to show a nonshrinking behavior at low temperatures.

In the range 28−36 °C, PNIPAM chains in both the outside and inside coronas of PS(207)-*b*-PNIPAM(176) vesicles overlap and collapse, leading to more rapid decreases of $\langle R_g \rangle$ and $\langle R_h \rangle$, as shown in Figure 6. At a temperature above ∼36 °C, PNIPAM chains in either outside or inside corona stop collapse, and $\langle R_h \rangle$ and $\langle R_g \rangle$ do not decrease anymore. Correspondingly, Figure 7 shows that $\langle R_g \rangle / \langle R_h \rangle$ gradually increases from 0.92 to 0.95 in the range 20−28 °C and more rapidly increases from 0.95 to 1.05 in the range 28−36 °C. This is because the interior of the vesicle becomes hollow due to the collapse of the PNIPAM chains in the inside corona; i.e., the vesicles becomes more hollow as temperature increases. At a temperature above ∼36 °C, $\langle R_g \rangle / \langle R_h \rangle$ tends to be a constant of ∼1.05 because PNIPAM chains stop collapsing. The conformation changes of PNIPAM chains in the coronas of the vesicles are schematically described in Figure 8.

Conclusion

We prepared thermosensitive polymeric micelles and vesicles in water with narrowly distributed polystyrene-*b*-poly(*N*-isopropylacrylamide) (PS-*b*-PNIPAM) diblock copolymers and studied the conformational changes of PNIPAM blocks in their coronas using laser light scattering. The study shows that the PNIPAM chains in the coronas form brushes. PNIPAM brushes in coronas of the micelles exhibit a broaden collapse transition from 24 to 34 °C with some second-order character relative to free PNIPAM chains, which agrees with the theoretical predictions about polymer brushes on a spherical surface. PNIPAM brushes consisting of the coronas of the vesicles show a broad transition from 28 to 36 °C with a shrinking in the range from 20 to 28 °C. The interchain overlapping of the dense brushes on the concave surface of the vesicle is thought to be responsible for the shrinking at a low temperature. The thermosensitive vesicles turn hollow with increasing temperature due to the collapse of PNIPAM chains in the inside corona. The thermosensitive vesicles may find some applications.

Acknowledgment. The financial support of the National Major Research Plan Projects (90303021) and The "Bai Ren" Project of The Chinese Academy of Sciences is gratefully acknowledged.

References and Notes

(1) Stockmayer, W. H. *Makromol. Chem.* **1960**, *35*, 54.
(2) Flory, P. J. *Principles of Polymer Chemistry*, Cornell University Press: Ithaca, NY, 1953.
(3) de Gennes, P. G. *J. Phys., Lett.* **1985**, *46*, L639.
(4) Grosberg, A. Y.; Nechaev, S. K.; Shakhnovich, E. I. *J. Phys., Lett.* **1988**, *49*, 2095.
(5) Pitard, E.; Orland, H. *Europhys. Lett.* **1998**, *41*, 467.
(6) Kuznetsov, Y. A.; Timoshenko, E. G.; Dawson, K. A. *J. Chem. Phys.* **1995**, *103*, 4807.
(7) Khalatur, P. G.; Khokhlov, A. R.; Mologin, D. A.; Reineker, P. *J. Chem. Phys.* **2003**, *119*, 1232.
(8) Maury-Evertsz, J. R.; Estevez, L. A.; Lopez, G. E. *J. Chem. Phys.* **2003**, *119*, 9925.
(9) Pande, V. S.; Grosberg, A. Y.; Tanaka, T. *J. Chem. Phys.* **1997**, *107*, 5118.
(10) Pereira, G. G.; Williams, D. R. M.; Napper, D. H. *Langmuir* **1999**, *15*, 906.
(11) Baulin, V. A.; Halpeirin, A. *Macromol. Theory Simul.* **2003**, *12*, 549.
(12) Anufrieva, E. V.; Volkenstein, M. V.; Gotlib, Yu. Ya.; Krakovyak, M. G.; Pautov, V. D.; Stepanov, V. V.; Skorokhodov, S. S. *Dokl. Akad. Nauk SSSR* **1972**, *207*, 1379.
(13) Sun, S. T.; Nishio, I.; Swislow, G.; Tanaka, T. *J. Chem. Phys.* **1980**, *73*, 5971.
(14) Park, I. H.; Wang, Q. W.; Chu, B. *Macromolecules* **1987**, *20*, 1965. Park, I. H.; Kim, J. H.; Chang, T. *Macromolecules* **1992**, *25*, 7300.
(15) Kayaman, N.; Gurel, E. E.; Baysal, B. M.; Karasz, F. E. *Macromolecules* **1999**, *32*, 8399.
(16) Nakata, M.; Nakagawa, T. *Phys. Rev. E* **1997**, *56*, 3338.
(17) Fujishige, S.; Kubota, K.; Ando, I. *J. Phys. Chem.* **1989**, *93*, 3311. Kubota, K.; Fujishige, S.; Ando, I. *J. Phys. Chem.* **1990**, *94*, 5154.
(18) Wu, C.; Zhou, S. Q. *Phys. Rev. Lett.* **1996**, *77*, 3053. Wu, C.; Wang, X. H. *Phys. Rev. Lett.* **1998**, *79*, 4092.
(19) Rička, J.; Meewes, M.; Nyffenegger, R.; Binkert, Th. *Phys. Rev. Lett.* **1990**, *65*, 657. Binkert, T.; Oberreich, J.; Meewes, M.; Nyffenegger, R.; Rička, J. *Macromolecules* **1991**, *24*, 5806.
(20) Tiktopulo, E. I.; Bychkova, V. E.; Rička, J.; Ptitsyn, O. B. *Macromolecules* **1994**, *27*, 2879. Tiktopulo, E. I.; Uversky, V. N.; Lushchik, V. B.; Klenin, S. I.; Bychkova, V. E.; Ptitsyn, O. B. *Macromolecules* **1995**, *28*, 7519.
(21) Graziano, G. *Int. J. Biol. Macromol.* **2000**, *27*, 89.
(22) Lozinsky, V. I.; Simenel, I. A.; Kulakova, V. K.; Kurskaya, E. A.; Babushkina, T. A.; Klimova, T. P.; Burova, T. V.; Dubovik, A. S.; Grinberg, V. Y.; Galaev, I. Y.; Mattiasson, B.; Khokhlov, A. R. *Macromolecules* **2003**, *36*, 7308.
(23) Barker, I. C.; Cowie, J. M. G.; Huckerby, T. N.; Shaw, D. A.; Souter, I.; Swanson, L. *Macromolecules* **2003**, *36*, 7765.
(24) Schild, H. G. *Prog. Polym. Sci.* **1992**, *17*, 163 and references therein.
(25) Alexander, S. *J. Phys. (Paris)* **1977**, *38*, 983.
(26) de Gennes, P. G. *Macromolecules* **1980**, *13*, 1069.
(27) Halperin, A.; Tirrell, M.; Lodge, T. P. *Adv. Polym. Sci.* **1991**, *100*, 31.
(28) Zhao, B.; Brittain, W. J. *Prog. Polym. Sci.* **2000**, *25*, 677.
(29) Zhulina, E. B.; Borisov, O. V.; Pryamitsyn, V. A.; Birshtein, T. M. *Macromolecules* **1991**, *24*, 140.
(30) Napper, D. H. *Steric Stabilization of Colloidal Dispersions*; Academic Press: New York, 1983.
(31) von Recum, H.; Okano, T.; Kim, S. W. *J. Controlled Release* **1998**, *55*, 121.
(32) Hoffman, A. S. *J. Controlled Release* **1987**, *6*, 297.
(33) Klein, J.; Kumacheva, E. *Science* **1995**, *269*, 816.
(34) Ista, L. K.; Perez-Luna, V. H.; Lopez, G. P. *Appl. Environ. Microbiol.* **1999**, *65*, 2552.
(35) Yakubov, G. E.; Loppinet, B.; Zhang, H.; Rühe, J.; Sigel, R.; Fytas, G. *Phys. Rev. Lett.* **2004**, *92*, 115501. Domack, A.; Prucker, S.; Rühe, J.; Johannsmann, D. *Phys. Rev. E* **1997**, *56*, 680.
(36) Karim, A.; Satija, S. K.; Douglas, J. F.; Ankner, J. F.; Fetters, L. J. *Phys. Rev. Lett.* **1994**, *73*, 3407.
(37) Balamurugan, S.; Mendez, S.; Balamurugan, S. S.; O'Brien, M. J., II; Lopez, G. P. *Langmuir* **2003**, *19*, 2545. Yim, H.; Kent, M. S. Mendez, S.; Balamurugan, S. S.; Balamurugan, S.; Lopez, G. P.; Satija, S. *Macromolecules* **2004**, *37*, 1994. Yim, H.; Kent, M. S.; Huber, D. L.; Satija, S.; Majewski, J.; Smith, G. S. *Macromolecules* **2003**, *36*, 5244.
(38) Zhu, P. W.; Napper, D. H. *Langmuir* **1996**, *12*, 5992. Zhu, P. W.; Napper, D. H. *J. Colloid Interface Sci.* **1996**, *177*, 489.
(39) Kidoake, S.; Ohya, S.; Nakayama, Y.; Matsuda, T. *Langmuir* **2001**, *17*, 2402.
(40) Shan, J.; Chen, J.; Nuopponen, M.; Tenhu, H. *Langmuir* **2004**, *20*, 4671. Nuopponen, M.; Ojala, J.; Tenhu, H. *Polymer* **2004**, *45*, 3643.

(41) Takei, Y. G.; Aoki, T.; Sanui, K.; Ogata, N.; Sakurai, Y.; Okano, T. *Macromolecules* **1994**, *27*, 6163.
(42) Zhang, J.; Pelton, R.; Deng, Y. *Langmuir* **1995**, *11*, 2301.
(43) Hu, T. J.; Gao, J.; Wu, C. *J. Macromol. Sci., Phys.* **2000**, *B39*, 407.
(44) Plunkett, M. A.; Wang, Z. H.; Rutland, M. W.; Johannsmann, D. *Langmuir* **2003**, *19*, 6837.
(45) Thang, S. H.; Chong, Y. K.; Mayadunne, R. T. A.; Moad, G.; Rizzardo, E. *Tetrahedron Lett.* **1999**, *40*, 2435. Goto, A.; Sato, K.; Tsujii, Y.; Fukuda, T.; Moad, G.; Rizzardo, E.; Thang, S. H. *Macromolecules* **2001**, *34*, 402.
(46) Zimm, B. H. *J. Chem. Phys.* **1948**, *16*, 1099.
(47) Chu, B. *Laser Light Scattering*, 2nd ed.; Academic Press: New York, 1991.
(48) Berne, B.; Pecora, R. *Dynamic Light Scattering*; Plenum Press: New York, 1976.
(49) Xia, J.; Dubin, P. In *Macromolecular Complexes in Chemistry and Biology;* Dubin, P., Bock, J., Davies, R. M., Schultz, D. N., Thies, C., Eds.; Spring-Verlag: New York, 1994; p 247.
(50) Luo, L.; Eisenberg, A. *J. Am. Chem. Soc.* **2001**, *123*, 1012. Peng, H. S.; Chen, D. Y.; Jiang, M. *Langmuir* **2003**, *19*, 10989.
(51) Burchard, W. In *Light Scattering Principles and Development;* Brown, W., Ed.; Clarendon Press: Oxford, 1996; p 439. Burchard, W.; Schmidt, M.; Stockmayer, W. H. *Macromolecules* **1980**, *13*, 1265.
(52) Douglas, J. P.; Roovers, J.; Freed, K. F. *Macromolecules* **1990**, *23*, 418. Vagberg, L. J. M.; Cogan, K. A.; Gast, A. P. *Macromolecules* **1991**, *24*, 1670.

MA048227S